Loricrin and NRF2 Coordinate Cornification

Yosuke Ishitsuka[1], Tatsuya Ogawa[2], Yoshiyuki Nakamura[2], Noriko Kubota[2], Yasuhiro Fujisawa[2], Rei Watanabe[1], Naoko Okiyama[2], Manabu Fujimoto[1], Dennis R. Roop[3] and Akemi Ishida-Yamamoto[4]

Cornification involves cytoskeletal cross-linkages in corneocytes (the brick) and the secretion of lipids/adhesion structures to the interstitial space (the mortar). Because the assembly of lipid envelopes precedes corneocyte maturation, loricrin is supposed to be dispensable for the protection against desiccation. Although the phenotypes of *Lor* knockout (LKO) mice are obscure, the antioxidative response on the KEAP1/NRF2 signaling pathway compensates for the structural defect in utero. In this study, we asked how the compensatory response is evoked after the defects are repaired. To this end, the postnatal phenotypes of LKO mice were analyzed with particular attention to the permeability barrier function primarily maintained by the mortar. Ultrastructural analysis revealed substantially thinner cornified cell envelopes and increased numbers of lamellar granules in LKO mice. Superficial epidermal damages triggered the adaptive repairing responses that evoke the NRF2-dependent upregulation of genes associated with lamellar granule secretion in LKO mice. We also found that corneodesmosomes are less degraded in LKO mice. The observation suggests that loricrin and NRF2 are important effectors of cornification, in which proteins need to be secreted, cross-linked, and degraded in a coordinated manner.

JID Innovations (2022);**2:**100065 doi:10.1016/j.xjidi.2021.100065

INTRODUCTION

The ultimate barrier function of the epidermis resides in the stratum corneum (SC) that is formed above the tight junction, an evolutionarily ancient paracellular diffusion barrier. The SC is often structurally compared with the bricks and mortar, which correspond to corneocytes and interstitial lamellated lipid, respectively (Nemes and Steinert, 1999). Loricrin (LOR) forms cornified cell envelopes (CEs) (Mehrel et al., 1990), a heavy disulfide (−S−S−)/ε-(γ-glutamyl) lysine cross-linked macromolecular structure that is formed inside the cell periphery (Rice and Green, 1977). Despite its quantitative significance, the gene knockout study of the epidermal thiol-rich protein revealed that LOR is dispensable for the epidermal permeability barrier as assessed by transepidermal water loss (TEWL) levels or the passive diffusion of the Lucifer yellow dye (Koch et al., 2000). These observations suggest that LOR does not affect the inside-out or the outside-in permeability barrier function. Nonetheless, Koch et al. (2000) found that *Lor* knockout (LKO) mice exhibit a delay in the development of the epidermal barrier formation in utero. The relative abundance of thiol (−SH) to disulfide (−S−S−) in the stratum granulosum (SG) appears to be primarily responsible for this delay because abundant thiol-reactive electrophiles, such as sulforaphane, in the amniotic fluid rescues the phenotype (Huebner et al., 2012). Mechanistically, sulfur-rich CE protein depletion activates the KEAP1/NRF2 signaling pathway (Yamamoto et al., 2018). Keratinocyte (KC) antioxidants, such as small proline-rich proteins (i.e., SPRRs) (Huebner et al., 2012) or late cornified envelopes (Ishitsuka et al., 2016), are massively incorporated in LKO CEs. Accordingly, inhibiting NRF2 DNA binding activity through the transgenic introduction of the dominant-negative *Nrf2*mutant abrogates the adaptive response, leading to lethal desiccation in LKO mice (Huebner et al., 2012). Because wild-type (WT) dominant-negative *Nrf2* mice are apparently healthy (Huebner et al., 2012), the observations suggest that LOR and the KEAP1/NRF2 system collectively promote cornification: cytoskeletal cross-linkage (the brick) and the paracellular secretion of lipids/adhesion structures (the mortar) (Eckhart et al., 2013). However, how the compensatory response is evoked and maintained in terrestrial conditions remains a matter of interest. To address this, we sought to further clarify the postnatal phenotypes in LKO mice with a particular focus on the SC permeability barrier function that primarily depends on the mortar.

RESULTS

LOR is mandatory for corneocyte maturation

According to the CE assembly model by Steinert et al. (Kalinin et al., 2001), LOR is a major CE reinforcement component (Mehrel et al., 1990) that organizes the cross-linkages of cytoskeletal proteins, such as suprabasal

[1]Department of Dermatology, Graduate School of Medicine, Osaka University, Osaka, Japan; [2]Department of Dermatology, Faculty of Medicine, University of Tsukuba, Tsukuba, Japan; [3]Department of Dermatology and Charles C. Gates Center for Regenerative Medicine, University of Colorado Anschutz Medical Campus, Aurora, Colorado, USA; and [4]Department of Dermatology, Asahikawa Medical University, Asahikawa, Japan

Correspondence: Yosuke Ishitsuka, Department of Dermatology, Graduate School of Medicine, Osaka University, 2-2 Yamadaoka, Suita, Osaka 565-0871, Japan. E-mail: ishitsuka@derma.med.osaka-u.ac.jp

Abbreviations: CD, corneodesmosome; CDSN, corneodesmosin; CE, cornified envelope; CE_i, immature/fragile cornified envelope; DKO, Lor−Nrf2 double knockout; DMF, dimethyl fumarate; K, keratin; KC, keratinocyte; LG, lamellar granule; LKO, Lor knockout; LOR, loricrin; NKO, Nrf2 knockout; SC, stratum corneum; SG, stratum granulosum; TEWL, transepidermal water loss; TS, tape-stripping; WT, wild type

Received 8 June 2021; revised 8 August 2021; accepted 20 August 2021; accepted manuscript published online XXX; corrected proof published online XXX

Cite this article as: JID Innovations 2022;2:100065

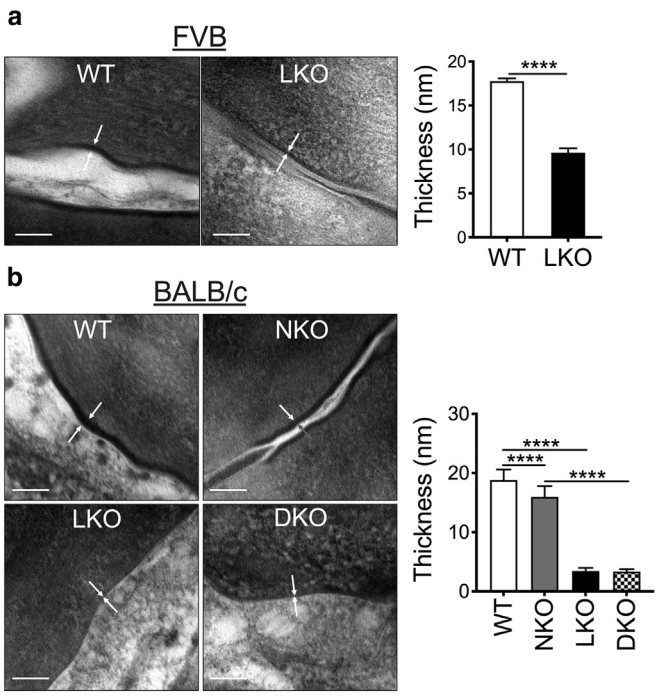

Figure 1. LOR is mandatory for corneocyte maturation. Neonatal back skin was subjected to TEM, and SC was observed at the first (SC1) and second (SC2) layers. (**a**) Representative TEM images from P0 WT and LKO neonatal back skin on the FVB background. Arrows indicate the cornified CEs. Bar = 100 nm. The CE thickness was measured at the SC2 under TEM. The results presented are from fields at a magnification of 15,000; n = 8, $^{****}P < 0.001$. (**b**) Representative TEM images from P0 WT, LKO, NKO, and DKO back skin on the BALB/c background. Arrows indicate the CEs. Bar = 100 nm. The CE thickness was measured at the SC2 under TEM. The results presented are from fields at a magnification of 15,000; n = 12; $^{***}P < 0.005$ and $^{****}P < 0.001$. CE, cornified envelope; DKO, *Nrf2*–*Lor* double knockout; LKO, *Lor* knockout; LOR, loricrin; NKO, *Nrf2* knockout; P0, neonatal; SC, stratum corneum; TEM, transmission electron microscopy; WT, wild type.

keratin (K) 1/K10 or FLG (Steinert and Marekov, 1995). A recent mass spectrometry–based study (Rice et al., 2016) and the photosensitive phenotype in LKO mice (Ishitsuka and Roop, 2018) support this view. Using transmission electron microscopy, CEs are observed as electron-dense deposits formed inside the cell periphery (Lavker and Matoltsy, 1970). Neonatal back skin from LKO mice on the FVB background was subjected to the ultrastructural evaluation, and it was revealed that their CEs were substantially thinner and less electron dense than those of WT mice (Figure 1a). We also performed a transmission electron microscopy study on the *Lor*–*Nrf2* double knockout (DKO) mice backcrossed into the BALB/c background, which exhibits gross phenotypes comparable with those of LKO mice, presumably because of the compensation by other NRF family members (Huebner et al., 2012). The CE thickness was consistently thinner in neonatal LKO/DKO mice regardless of their genetic background. It is noteworthy that neonatal *Nrf2* knockout (NKO) mice harbored significantly thinner electron-dense areas than WT mice (Figure 1b), suggesting that NRF2 is a critical effector of keratinization (Schäfer et al., 2012; Wakabayashi et al., 2003). Together, these findings indicate that LOR is a major CE protein that promotes corneocyte maturation.

SC paracellular barrier structure in LKO epidermis

Before LOR completes disulfide (−S−S−)-mediated cytoskeletal cross-linkages, the corneocyte outer coat, termed corneocyte lipid envelopes, is formed (Nemes and Steinert, 1999; Swartzendruber et al., 1987). Specifically, the ε-(γ-glutamyl) lysine isopeptide bond–mediated cross-linkage of the three scaffolding components envoplakin, periplakin, and involucrin is indispensable for corneocyte lipid envelopes formation (Sevilla et al., 2007). However, at this point of the CE assembly, corneocyte maturation is incomplete, and CEs remain immature/fragile (immature/fragile cornified envelope [CE_f]) (Michel et al., 1988), considering the relative abundance of the earlier scaffolding components, as in the psoriatic epidermis (Ishida-Yamamoto et al., 1996) or LKO mice (Ishitsuka and Roop, 2018; Koch et al., 2000; Rice et al., 2016). Because the psoriatic epidermis, which harbors CE_f (Ishida-Yamamoto et al., 1996; Michel et al., 1988), exhibits increased lamellar granule (LG) numbers (Ghadially et al., 1996), one could compare that LKO mice increase the LG storage. Indeed, we found an increase in cytoplasmic LG numbers in FVB neonatal LKO mice (Figure 2), whereas the areas of secreted LGs were significantly smaller in LKO mice (Figure 3). This change was accompanied by increased transcripts and proteins of ABCA12, which is essential for LG biogenesis and secretion (Zuo et al., 2008), in the neonatal mice on both backgrounds (Figure 4, data not shown). With respect to the effects of NRF2 on LG biogenesis, NKO mice harbored significantly increased LG numbers compared with that for WT mice, whereas LG numbers were not significantly decreased in DKO mice compared with those in LKO mice (Figure 3b), suggesting that NRF2 may not affect LG biogenesis per se. However, it is noteworthy that the structure of SC lamellae remained undisturbed in LKO mice, unlike psoriatic epidermis (Ghadially et al., 1996). These observations suggest that LOR is nonessential for the SC permeability barrier function (Koch et al., 2000) primarily maintained by the biogenesis and secretion of LGs.

Desmosomal plaque proteins, such as desmoplakin, are incorporated into the CE through ε-(γ-glutamyl) lysine cross-linkage during the scaffolding phase (Nemes and Steinert, 1999), and the modified desmosome corneodesmosomes (CDs) replace the living layer–type adhesion structure (Ishida-Yamamoto et al., 2018, 2011). Therefore, LG-derived CDs preferentially bind to the immature CE_f (Allen et al., 2001; Serre et al., 1991) in advance of corneocyte maturation (Hohl et al., 1991; Mehrel et al., 1990) and shedding (Jonca et al., 2002; Serre et al., 1991; Simon et al., 2001, 1997). The deficiency of CD protein corneodesmosin (CDSN) (Leclerc et al., 2009; Matsumoto et al., 2008) as well as its premature proteolysis (Descargues et al., 2005) lead to lethal desmosomal defects in mice. The transcripts of *Cdsn* were significantly increased in LKO mice compared with those in WT or DKO mice (Figure 4). Accordingly, the numbers of undegraded CDs were significantly higher in LKO mice than in WT mice (Figures 5 and 6). Although the previous study revealed an increased incorporation of desmoglein 1 into the detergent/reductant-insoluble fraction (isolated CEs) in LKO epidermis (Rice et al., 2016), the transmission electron microscopy analysis did not reveal

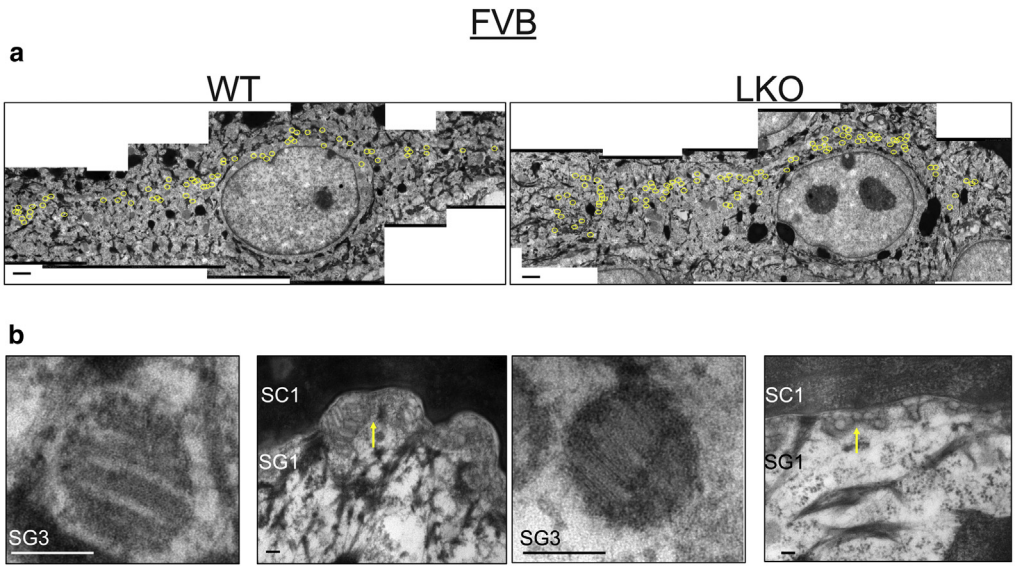

Figure 2. LGs in the absence of LOR. Neonatal back skin samples were subjected to TEM. (**a**) Representative TEM images in FVB neonatal mice. Yellow circles indicate the cytoplasmic LGs in the lowermost SG3. Bar = 1 μm. (**b**) Left: Cytoplasmic LGs in the SG3, high magnification. Right: Secreted LGs (yellow arrows, between the uppermost SG [SG1] and the lowermost layer of the stratum corneum [SC1]). Bar = 100 nm. LG, lamellar granule; LKO, *Lor* knockout; LOR, loricrin; SC, stratum corneum; SG, stratum granulosum; TEM, transmission electron microscopy; WT, wild type.

apparent numerical changes in desmosomes in the stratum spinosum (data not shown). Therefore, it is the enhanced LG secretion rather than the increased desmosomes that appears to be primarily responsible for the numerical changes of CDs. However, in contrast to the LG numbers, CDs remained undegraded in LKO and DKO mice compared with those in WT and NKO mice, respectively. The C-terminus of CDSN (Jonca et al., 2002) undergoes disulfide (−S−S−) cross-linkage to CEs (Hohl et al., 1991; Simon et al., 2001, 1997) concurrently with serine protease–mediated proteolytic cleavage on the N-terminus (Simon et al., 2001, 1997). Therefore, these observations suggest that LOR modifies the stability of CDSN during cornification. To address this, the protein extracts from heat-split neonatal epidermis, using SDS buffer that contained a reducing agent (β-mercaptoethanol), were subjected to immunoblotting using an anti-CDSN antibody recognizing the N-terminus. LKO/DKO mice exhibited stronger bands of undegraded CDSN (40–48 kDa) (Simon et al., 2001) than WT/NKO mice (Figure 6c). These results suggest that it is LOR, not the transcription factor NRF2, that promotes CD processing by enhancing disulfide (−S−S−) cross-linkage.

NRF2 promotes LG secretion

Neonatal mice undergo adaptive responses on commencing a terrestrial life (Huebner et al., 2012), and we found that neonatal LKO mice exhibited increased levels of *Abca12* and *Cdsn* transcripts in an NRF2-dependent manner (Figure 4). Because tissue regeneration mimics organ development (Wood et al., 2002), the repairing responses after the abrasion of differentiated epidermal layers (Gregorio et al., 2010) could recapitulate the development in utero (Huebner et al., 2012; Ishitsuka et al., 2016). Adult BALB/c mice were subjected to a tape-stripping (TS) procedure, and the dependence of LKO mice on the transcription factor NRF2 was analyzed. When compared with DKO mice, LKO mice exhibited significantly increased levels of *Abca12*/*Cdsn* transcripts, in addition to NAD(P)H quinone dehydrogenase

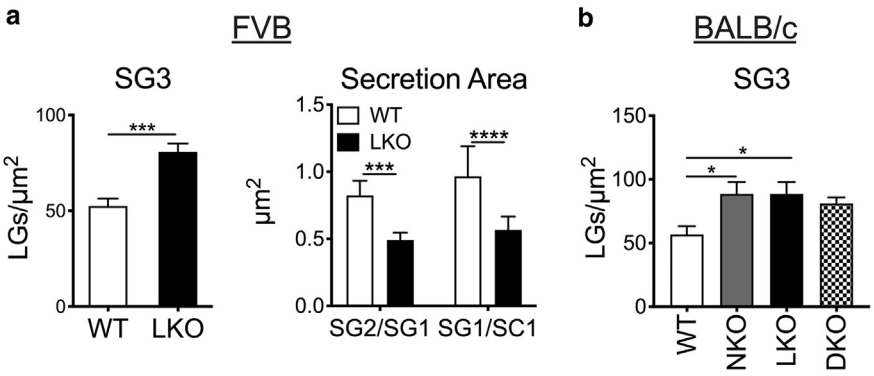

Figure 3. Increased LG numbers in the absence of LOR. Neonatal back skin samples were subjected to TEM. (**a**) The number of LGs in the SG3 per μm^2 of the cytoplasmic area in neonatal FVB mice; n = 8; $^{***}P < 0.005$. The secretory area of LG was quantified at a magnification of 3,000 with a width of 5 μm. SG2/SG1, between the second and uppermost SG; SG1/SC1, between the SG1 and SC1. n = 8; $^{****}P < 0.001$. (**b**) The number of LGs in the SG3 per μm^2 of the cytoplasmic area in the BALB/c neonatal mice. n = 8; $^{*}P < 0.05$. DKO, *Nrf2*−*Lor* double knockout; LG, lamellar granule; LOR, loricrin; NKO, *Nrf2* knockout; SC, stratum corneum; SG, stratum granulosum; TEM, transmission electron microscopy; WT, wild type.

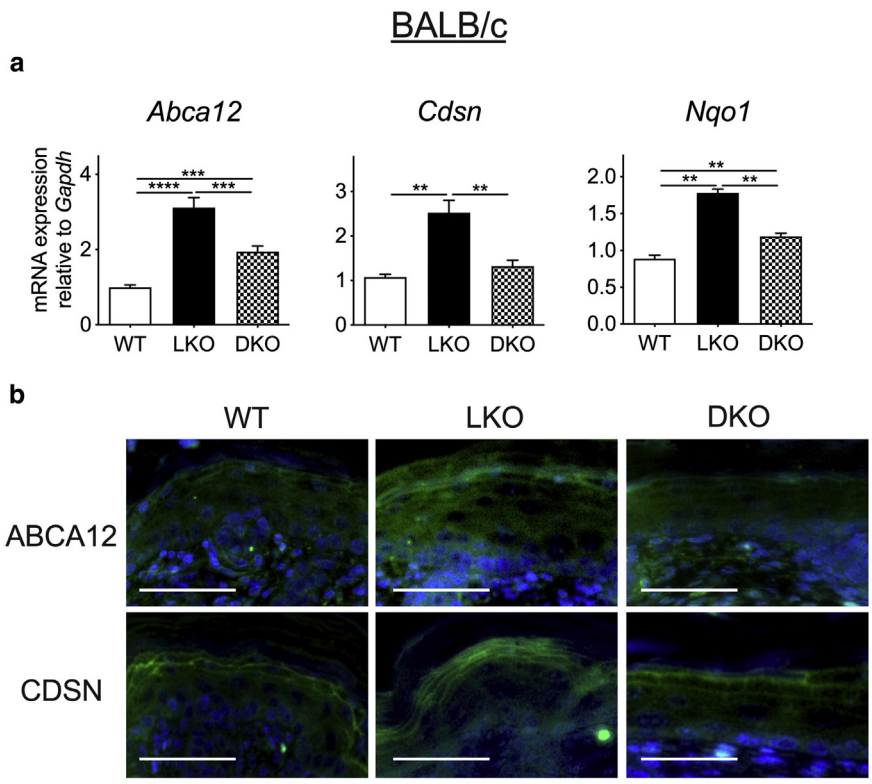

Figure 4. NRF2-dependent upregulation of lamellar granule markers in LKO epidermis. Samples from full-thickness neonatal back skin were collected in neonatal BALB/c mice. (**a**) Real-time PCR analysis was conducted. n = 6 for each genotype; $^{**}P < 0.01$, $^{***}P < 0.005$, and $^{****}P < 0.001$. (**b**) Representative immunofluorescence staining of ABCA12 and CDSN. CDSN staining represents the N-terminus, which is supposed to be degraded during cornification. Bar = 50 μm. CDSN, corneodesmosin; LKO, *Lor* knockout; NKO, *Nrf2* knockout; WT, wild type.

1 (*Nqo1*) (Figure 7). Thus, the activation of the KEAP1/NRF2 system in LKO mice may represent endogenous adaptive responses against minor epidermal damages or defects.

We have characterized the importance of the KEAP1/NRF2 signaling pathway in the recovery of epidermal barrier function after primary inflammatory assaults, such as psoriasiform tissue reaction (Ogawa et al., 2020a). The recovery rates of TEWL levels could correspond to the efficiency of LG secretion (Menon et al., 1992) rather than biogenesis itself (Ghadially et al., 1996). To address this, we quantified the areas of LGs secreted into the interstitial space in neonatal mice. In contrast to neonatal FVB mice (Figure 3a), we found that BALB/c neonatal mice exhibited a substantial increase in the secretory areas during cornification, that is, migration from SG2/SG1 (between the second and uppermost SG) to SG1/SC1 (between the SG1 and SC1) (Figure 8a). This increase was abrogated in NKO/DKO mice, compared with that in WT/LKO mice (Figure 8a and b), suggesting that NRF2 promotes LG secretion. Correspondingly, adult NKO/DKO mice exhibited significantly decreased recovery rates of TEWL following the controlled TS procedure (Kuo et al., 2013), although both adult WT and LKO mice showed comparable recovery rates (Figure 8c). An electrophile dimethyl fumarate (DMF) was orally administrated to LKO and DKO mice to exogenously activate the KEAP1/NRF2 signaling pathway (Yamamoto et al., 2018). As was observed in the imiquimod-induced psoriasiform tissue reaction (Ogawa et al., 2020a), DMF treatment resulted in a more prompt recovery than vehicle treatment (Figure 8d). DKO mice also responded to the treatment to some extent, presumably depending on the NRF2-independent pathway (Schulze-Topphoff et al., 2016), which was also observed in the imiquimod setting (Ogawa et al., 2020a). However, the recovery responses in DMF-treated DKO mice remained slow compared with that in LKO mice (Figure 8d).

DISCUSSION

Cell-autonomous activation of NRF2 in LKO mice

The LG-mediated transport of lipids protects terrestrial mammals from desiccation (Nemes and Steinert, 1999), and that of the adhesion molecule CDSN maintains corneocyte cohesion and desquamation (Jonca et al., 2002; Leclerc et al., 2009; Matsumoto et al., 2008). The KEAP1/NRF2 signaling pathway induces SPRR2s (Huebner et al., 2012) or LCEs (Ishitsuka et al., 2016) during epidermal tissue development to compensate for the loss of LOR. In accordance with previous reports, the thinner electron-dense deposits in LKO corneocytes underscore the primary function of LOR as a major CE protein by promoting disulfide (−S−S−)-mediated cytoskeletal cross-linkages on exposure to ambient air (Hohl et al., 1991; Mehrel et al., 1990). Therefore, the upregulated expression levels of *Abca12* and *Cdsn* in LKO mice could be an NRF2-dependent, cell-autonomous recovery response reinforcing the SC permeability barrier (Huebner et al., 2012). Our results may offer an explanation to the very different consequences resulting from the activated KC reduction–oxidation signaling in the epidermis; constitutive activation leads to pathologic hyperkeratosis (Schäfer et al., 2014, 2012; Wakabayashi et al., 2003), whereas timely signaling in LKO mice results in the development of a very mild phenotype (Schäfer and Werner, 2015).

However, what is the cause of the NRF2-mediated adaptive responses in LKO epidermis? The lack of the

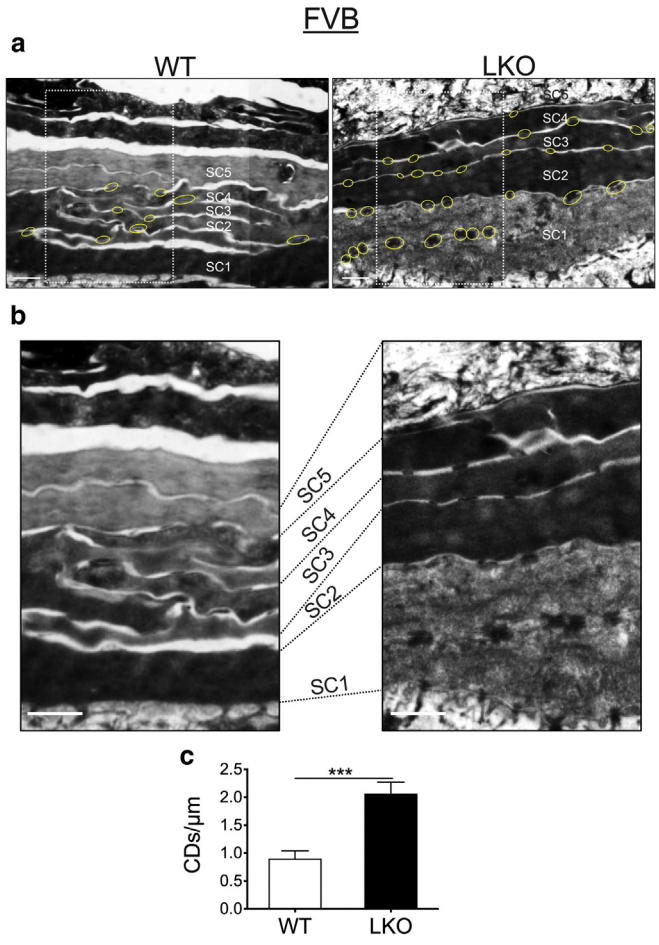

Figure 5. Undegraded corneodesmosomes in FVB LKO epidermis. (**a**) Representative ultrastructural images of the first layer of the SC1 to the fifth layer SC5 in the FVB P0 mice. Yellow circles indicate the undegraded CDs. Bar = 1 μm. (**b**) Higher magnification of the areas enclosed with the dotted line in **a**. (**c**) The number of undegraded CDs was measured from the SC1 to the SC5 after generating montages at a magnification of 15,000 with a width of 20 μm. n = 6 ***$P < 0.005$. CD, corneodesmosome; LKO, —*Lor* knockout; P0, neonatal; SC, stratum corneum; WT, wild type.

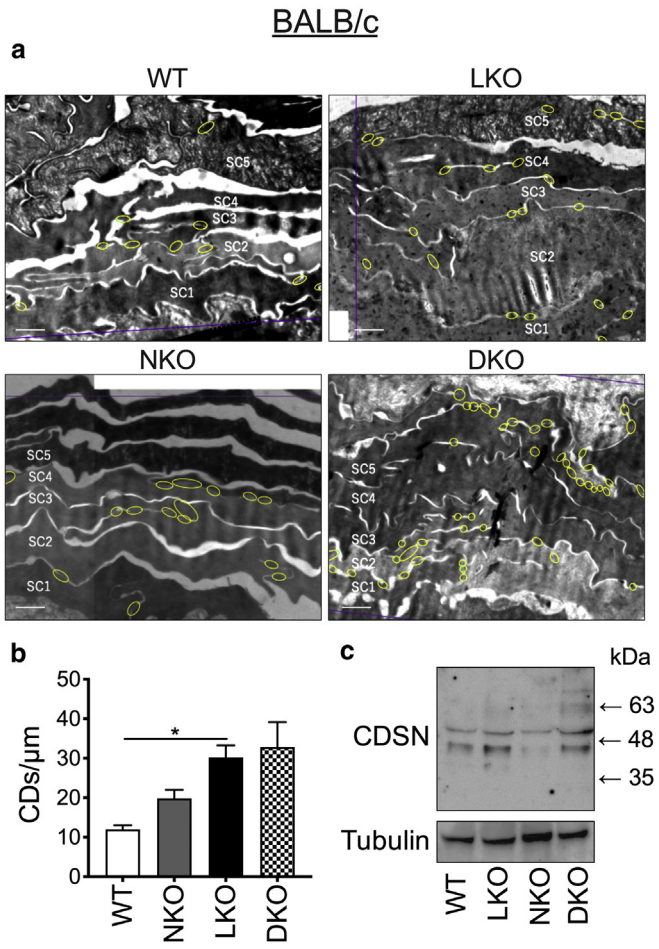

Figure 6. Undegraded CDs in BALB/c *Lor/Nrf2*-knockout epidermis. (**a**) Representative ultrastructural images of the SC1 to the SC5 in the BALB/c P0 mice. Yellow circles indicate the undegraded CDs. Bar = 1 μm. (**b**) The number of undegraded CDs was quantified from the SC1 to the SC5 after generating montages at a magnification of 15,000 with a width of 20 μm. n = 6 ***$P < 0.005$. (**c**) Heat-split epidermis from P0 BALB/c mice was solubilized in a buffer containing 2% SDS and 25 mM β-mercaptoethanol. The lysates were subjected to immunoblotting using the anti-CDSN antibody recognizing the N-terminus subjected to serine protease–mediated proteolysis. CD, corneodesmosome; CDSN, corneodesmosin; DKO, *Nrf2*—*Lor* double knockout; LKO, *Lor* knockout; NKO, *Nrf2* knockout; P0, neonatal; SC, stratum corneum; WT, wild type.

sulfur-rich structural protein would profoundly affect the epidermal sulfur metabolism in LKO SG, that is, the formation of disulfide (—S—S¬—) cross-linkages (Van Scott and Flesch, 1954). Therefore, it is most likely that the thiol-laden cytoskeleton-associated protein KEAP1 (Dinkova-Kostova et al., 2002; Kang et al., 2004) senses the cytoplasmic reduction–oxidation imbalance, and its conformational changes disrupt the phylogenetically ancient interaction with the effector protein NRF2 (Itoh et al., 1999; Katoh et al., 2005; Kobayashi et al., 2002) during the upward migration of KCs. As a consequence, antioxidative SPRRs (Vermeij and Backendorf, 2010; Vermeij et al., 2011) are massively induced, albeit LKO CE_f (Koch et al., 2000; Michel et al., 1988). The biochemical properties of LKO CEs may allow the easier attachment of the LG content (Ishida-Yamamoto et al., 1996; Rice et al., 2016) and prevent the detrimental activation of NRF2. Therefore, the reduction–oxidation–driven backup or repairing response in LKO mice resembles the self-righting system of the sailboat. In short, the truncated epidermal differentiation program in LKO epidermis may be a tissue-intrinsic cue that directs recovery from the primary injury (Ishitsuka et al., 2020; Ogawa et al., 2020a), and the KEAP1/NRF2 signaling pathway is a major regulator of such adaptive tissue responses (Huebner et al., 2012; Ishitsuka et al., 2016). Although the oxidative amniotic milieu promotes disulfide (—S—S—) cross-linkages and assists the maturation of LKO CEs, the consequences of dominant-negative *Nrf2* transgene introduction in LKO mice must be cautiously interpreted (Huebner et al., 2012) because the mutant *Nrf2* primarily abrogates the cell-autonomous adaptive responses.

LOR and desquamation

Another important but rather unexpected finding was the retention of undegraded CDs in the LKO SC. The absence of CDSN (Leclerc et al., 2009; Matsumoto et al., 2008) or aberrantly activated serine protease activity lymphoepithelial

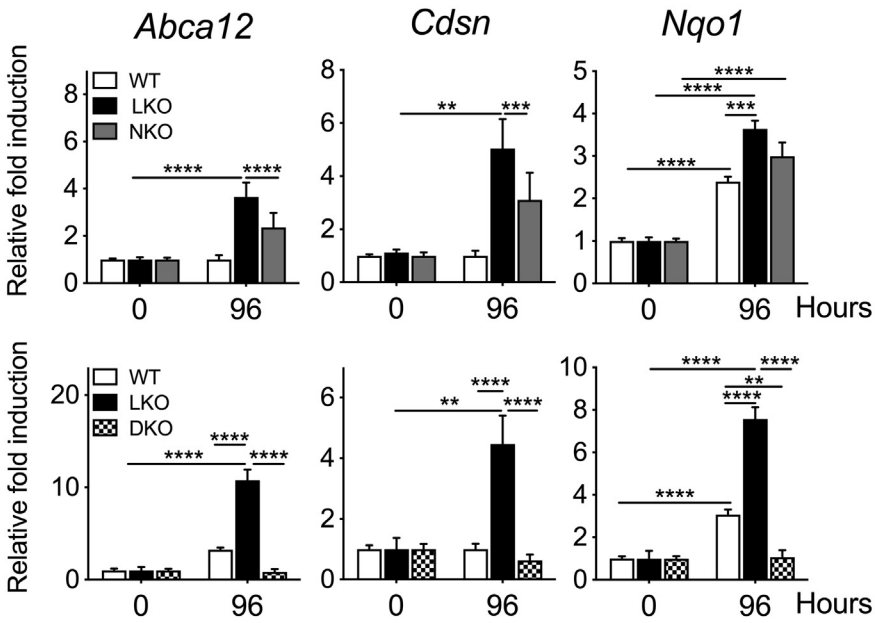

Figure 7. NRF2-dependence of the repairing responses in adult LKO mice. TS was performed on the depilated back skin of adult BALB/c mice. The skin samples were collected immediately after depletion (0 hours) or 96 hours after TS and were subjected to real-time PCR analysis. The results are from at least four independent mice per experiment, and the results from two independent experiments are shown. n = 6 for each experimental group; $^{**}P < 0.01$, $^{***}P < 0.005$, $^{****}P < 0.001$. DKO, *Nrf2−Lor* double knockout; LKO, *Lor* knockout; NKO, *Nrf2* knockout; TS, tape stripping; WT, wild type.

Kazal-type related inhibitor deficiency (Descargues et al., 2005) leads to premature SC detachment and severe desmosomal defects. LGs contain the serine protease kallikreins (Ishida-Yamamoto et al., 2005) that break down CDs. Although LGs secrete both kallikreins and lymphoepithelial Kazal-type related inhibitor (Ishida-Yamamoto et al., 2005), the results suggest that disulfide (−S−S−)-rich LOR directly interacts with CDSN and modifies its structure in the upper SC, as previously indicated (Mils et al., 1992; Serre et al., 1991; Simon et al., 2001, 1997). After secretion, the kallikrein-mediated proteolytic cleavage of CDSN begins from the *N*-terminus, which is responsible for its homophilic adhesive property (Jonca et al., 2002). By contrast, the C-terminus remains undegraded and covalently binds to CEs through disulfide (−S−S−) cross-linkages (Simon et al., 2001). Similar to the CE_f (Allen et al., 2001; Michel et al., 1988; Serre et al., 1991), LKO CEs may promote CDSN attachment to corneocytes. However, impaired CE disulfide (−S−S−) cross-linkages may prevent the structural maturation of CDs and thus proteolytic cleavage in the absence of LOR (Hohl et al., 1991; Huebner et al., 2012; Ishitsuka and Roop, 2018; Mehrel et al., 1990; Rice et al., 2016; Vermeij and Backendorf, 2010; Vermeij et al., 2011). Our previous observations may support that LKO corneocytes harbor abundant uncross-linked FLG that yields natural moisturizing factors (Ishitsuka and Roop, 2018), and the deficiency of the humectant could augment kallikrein proteolytic activity (Ishida-Yamamoto et al., 2018, 2011).

These observations highlight previously unappreciated functions of LOR because LOR may coordinate desquamation. Although we have not determined why delayed CD processing does not cause substantially thickened SC in LKO mice, as observed in the psoriatic (Allen et al., 2001; Simon et al., 2008) or palmoplantar (Mils et al., 1992; Serre et al., 1991) epidermis, these results suggest that LOR provides the structural basis of desquamation, which is hardwired into the epidermal differentiation program.

Evolutional significance of LOR

Overall, LOR is dispensable for the protection against desiccation per se, unless it acquires nuclear-localizing signals and moves to the nucleus (Ishida-Yamamoto et al., 2000; Suga et al., 2000). The nuclear-localizing signal-harboring mutant *LOR* gene disturbs the SC permeability barrier, as assessed by the TEWL levels or the passive diffusion of the Lucifer yellow dye, irrespective of the presence or absence of WT LOR (Suga et al., 2000).

Consequently, what is LOR for? Similar to the salivary PRP, the alternative CE constituent SPRRs are structurally less organized (Williamson, 1994). The biochemical property of the PRP is advantageous in counteracting the harmful effects of xenobiotics, such as plant polyphenols (tannins) (Williamson, 1994). Furthermore, the high cysteine content of SPRRs allows the efficient quenching of ROS (Vermeij and Backendorf, 2010; Vermeij et al., 2011). By contrast, the primary protein structure of LOR favors intramolecular/intermolecular disulfide cross-linkages in vivo (Hohl et al., 1991; Mehrel et al., 1990). This biochemical peculiarity renders the purification of the native LOR protein in the exogenous gene expression system as significantly harder (Vermeij et al., 2011) as described in another cytoskeletal thiol-laden protein KEAP1 (Dinkova-Kostova et al., 2002).

The differentiation of cutaneous tissue highly depends on the gene expression program of the KCs, and tissue imprinting endows the isolated KCs with phenotypes peculiar to their tissue origin. Neither corneal KCs nor esophageal KCs are able to differentiate into the SC (Doran et al., 1980). However, epidermal KCs do not differentiate into fully matured corneocytes when kept in submerged cultures, and the in vitro CEs (Rice and Green, 1977) do not contain as much amount of LOR as the epidermal CEs in vivo (Steinert et al., 1998). Because the in vitro CEs resemble the CE_f (Michel et al., 1988; Steinert et al., 1998) because they are abundant with IVL (Simon and Green, 1984) or SPRRs (Steinert et al., 1998), LKO CEs may represent an aquatic

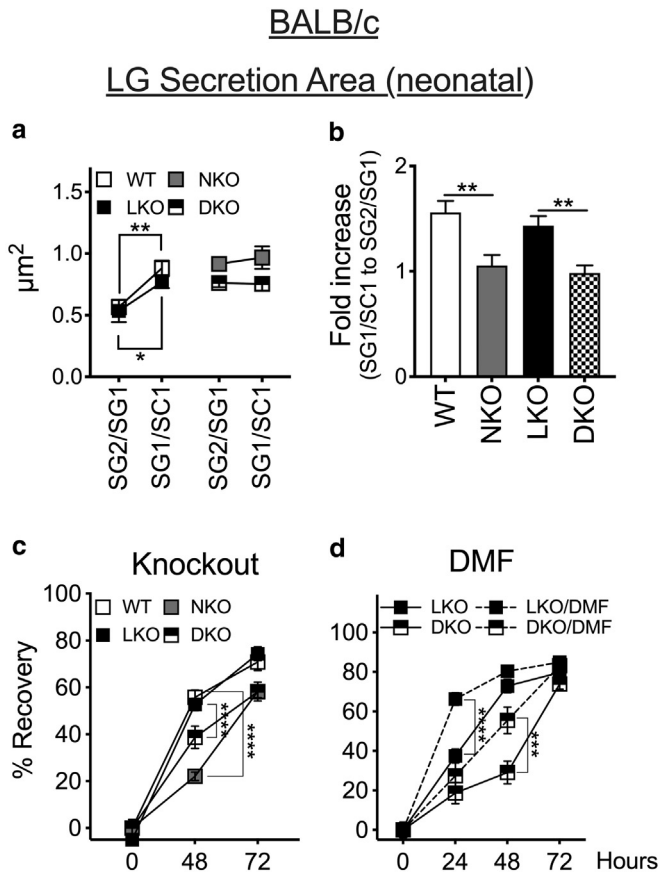

Figure 8. NRF2 promotes LG secretion. (**a, b**) The ultrastructural observations on the BALB/c P0 mice. (**a**) The secretory area of LG was quantified at a magnification of 3,000 with a width of 5 μm. SG2/SG1, between the second and uppermost SG; SG1/SC1, between the SG1 and the SC1. n = 13; $*P < 0.05$ and $**P < 0.01$. (**b**) The fold increase of LG secretory areas between SG2/SG1 and SG1/SC1 was calculated; n =13, $**P < 0.01$. (**c, d**) TEWL levels were measured after TS on the depilated back skin of adult BALB/c mice. The efficacy of LG secretion was determined as the percentage of recovery of TEWL levels compared with the baseline levels (immediately after the removal of the SC). (**c**) The recovery rates were analyzed in WT, LKO, NKO, and DKO mice. n = 8 for each genotype, $****P < 0.001$. (**d**) TS was performed on adult LKO and DKO mice under the intervention with the electrophile DMF. The solid line indicates LKO or DKO with vehicle treatment; the dashed line indicates LKO or DKO with DMF treatment. n = 8 for each experimental group; $***P < 0.005$ and $****P < 0.001$. DKO, *Nrf2–Lor* double knockout; DMF, dimethyl fumarate; LG, lamellar granule; LKO, *Lor* knockout; NKO, *Nrf2* knockout; P0, neonatal; SC, stratum corneum; SG, stratum granulosum; TEWL, transepidermal water loss; WT, wild type.

pattern of epidermal differentiation. Indeed, the phylogenetic analysis revealed that the K1/K10 pair, which partner with LOR through disulfide (–S–S–) cross-linkages (Rice et al., 2016), is deleted from the keratin gene cluster in cetaceans (Ehrlich et al., 2019). Analogous to the psoriatic epidermis harboring the CE_f (Ishida-Yamamoto et al., 1996; Michel et al., 1988), the dolphin epidermis expresses stress or hyperproliferation-associated K6/K17 (Ehrlich et al., 2019), which are also abundant in neonatal LKO CE (Rice et al., 2016; unpublished observations).

The decreased sulfur content in the LKO epidermis presumably makes the differentiating epidermal layers susceptible to NRF2 activation and may enhance the LG-mediated secretion of peptidases/peptidase inhibitors, such as secretory leukocyte peptidase inhibitor (Schäfer et al., 2012). The adaptive response becomes evident particularly when superficial epidermal damages are present, as observed in ichthyoses (Schäfer et al., 2012; Wakabayashi et al., 2003), psoriasis (Ogawa et al., 2020a), or atopic dermatitis (Ogawa et al., 2020b). In accordance with our previous works (Ishitsuka and Roop, 2020; Ishitsuka et al., 2020), we would like to conclude that LOR and NRF2 serve as important effectors of cornification, in which proteins need to be secreted, cross-linked, and degraded in a coordinated manner.

MATERIALS AND METHODS

Mice

All mice used in this study were maintained under specific pathogen-free conditions at the animal facility of the University of Tsukuba, and all procedures were approved by the University of Tsukuba Ethics Committee. LKO mice were maintained on the FVB background and backcrossed into the BALB/c background (Charles River Laboratories, Wilmington, MA) using DartMouseTM speed congenic service (a BALB/c content percentage >99% was confirmed). Separately, NKO mice on a BALB/c background were obtained from the Riken BioResource Research Center (Tsukuba, Japan) (Itoh et al., 1997) and crossed with the BALB/c LKO mice. WT mice were purchased from Charles River Laboratories (Yokohama, Japan). Age-matched mice (aged 8–12 weeks) were randomly selected from a pool for experiments housed in the same colony.

Transmission electron microscopy

The samples from neonatal back skin were fixed in half-strength Karnovsky fixative, followed by further fixation in 1% osmium tetroxide in distilled water. After en bloc staining with uranyl acetate, specimens were dehydrated in ethanol and embedded in Epon812 (Taab, Berkshire, United Kingdom). Ultrathin sections were stained with uranyl acetate and lead citrate.

To count CDs or LGs, montages were prepared using Adobe Photoshop, version 6.0 (Adobe Systems, San Jose, CA) at a magnification of 150,000, as described in a previous study (Igawa et al., 2011). We counted undegraded CD components in the lowermost SC layer (SC1) to the fifth SC layer (SC5) or cytoplasmic LGs in the SG3. All analyses were performed on at least four mice of each genetic background.

TS-mediated abrasion of differentiated epidermal layers

The back skin of adult mice was depilated (Epilat; Kracier, Tokyo, Japan). TS was performed using 20 strokes of a book tape (Scotch; 3M, Tokyo, Japan) across the back, as described previously (Gregorio et al., 2010). The back skin was collected for histological/expression analysis at the indicated time points. For TEWL measurement, TS was conducted using an adhesive tape (CELLOTAPE; Nichiban, Tokyo, Japan), as previously described (Kuo et al., 2013). The tape was carefully attached to the middle back skin, and SC was gently removed using four or five strokes. This typically resulted in spots of punctate hemorrhage and increased the TEWL to 100 ± 15 gm^{-2}/h; afterward, we recorded the recovery response for up to 96 hours. The TEWL from the skin surface was measured at room temperature (22–25 °C) at 40–60% humidity with a VAPOSCAN AS-VT100RS system (ASCH Japan, Tokyo, Japan). Individual values were compiled as two consecutive measurements on the same site on at least two independent sites on the back. The recovery response was indicated as percentage recovery rates of TEWL levels to the

baseline (measured immediately after depilation). DMF (242926; Sigma-Aldrich, St. Louis, MO) was diluted in 200 μl of 0.1% Methocel/water (Fujifilm Wako Pure Chemical, Osaka, Japan) and administered by oral gavage starting from 3 hours before TS until the end of TEWL measurement. The mice received DMF (15 mg/kg) or the vehicle control (Methocel/water) twice a day.

Quantitative real-time reverse transcriptase PCR

Pieces of full-thickness neonatal back skin of BALB/c mice were collected and homogenized in TRIzol reagent (15596-026; Thermo Fisher Scientific, Waltham, MA), and the total RNA was isolated. cDNA was then synthesized using a high-capacity cDNA reverse transcription kit (4368814; Thermo Fisher Scientific). The primers specific to each target with double-quenched probes, which were purchased from the Integrated DNA Technologies (Coralville, IA) Primetime Predesigned Library, were as follows: Mm.PT.58.5645042 for *Abca12*, Mm.PT.58.6164239 for *Cdsn*, and Mm.PT.58.10871473 for *Nqo1*. The primers for *Gapdh* (4352339E; Thermo Fisher Scientific) were used as an internal reference. The data were analyzed using the QuantStudio 5 Real-Time PCR System (Thermo Fisher Scientific). QRT-PCR data were interpreted using the comparative CT method (ΔΔCT method).

Immunofluorescence staining

The skin samples were fixed with 10% buffered formalin overnight. After paraffin embedding, 3-μm sections were deparaffinized and subjected to antigen retrieval and blocking with PBS (pH 7.2) containing 10% goat serum, followed by 3 hours of incubation at room temperature with diluted primary antibodies (ABCA12, 2 μg/ml, bs-11906R; Bioss, Woburn, MA; CDSN, 4.7 μg/ml, 27953-1-AP; Proteintech, Rosemont, IL). Antibody binding was visualized by incubation with a secondary antibody (anti-rabbit IgG-FITC, 2 μg/ml, sc-2012; Santa Cruz Biotechnology, Santa Cruz, CA) for 60 minutes at room temperature, followed by mounting with medium containing DAPI (VECTASHIELD mounting medium with DAPI, H-1200; Vector Laboratories, Burlingame, CA). The samples were examined using a fluorescence microscope (BZ-X710; Keyence, Osaka, Japan).

Immunoblotting

Epidermal sheets were prepared from neonatal BALB/c mice by heat separation, as previously described (Macdiarmid and Wilson, 2001), and snap frozen for storage. The sheets were then lysed in SDS buffer (Tris-hydrogen chloride [pH 6.8], 2% SDS, 10% glycerol) with 25 mM β-mercaptoethanol. Protein concentration was estimated using a BCA protein assay (23225; Thermo Fisher Scientific). Equal amounts of protein were subjected to Tris-SDS-PAGE on a 4–20% acrylamide gel (4561096; Bio-Rad, Hercules, CA) and transferred onto 0.22-μm pore nitrocellulose membranes (10600001; GE Healthcare, Buckinghamshire, United Kingdom). The membranes were incubated overnight with the following primary antibodies: anti-CDSN (4.7 μg/ml, 25973-1-AP; Proteintech) and anti-tubulin (1 μg/ml, 017-25031; Fujifilm Wako Pure Chemical), followed by a 60-minute incubation with horseradish peroxidase–labeled secondary antibodies against rabbit or mouse IgG (0.04 μg/ml, sc-2004 or sc-2005; Santa Cruz Biotechnology). Antibody binding was visualized and enhanced with SuperSignal West Dura Extended Duration Substrate (34075; Thermo Fisher Scientific) and an image analysis system (LAS4000 Mini; Fujifilm Wako Pure Chemical).

Statistical analysis

Data were expressed as mean ± SEM. Comparisons were conducted using the Mann–Whitney U test (between two groups) or two-way ANOVA (time course/grouped experiments) using Prism 6 software (GraphPad Software, San Diego, CA). In all analyses, $P < 0.05$ was considered statistically significant.

Data availability statement

No datasets were generated or analyzed during this study.

ORCIDs

Yosuke Ishitsuka: http://orcid.org/0000-0001-9611-3090
Tatsuya Ogawa: http://orcid.org/0000-0001-6448-9747
Yoshiyuki Nakamura: http://orcid.org/0000-0003-2080-3049
Noriko Kubota: http://orcid.org/0000-0002-6050-680X
Yasuhiro Fujisawa: http://orcid.org/0000-0003-3010-8496
Rei Watanabe: http://orcid.org/0000-0001-8254-9176
Naoko Okiyama: http://orcid.org/0000-0002-5398-0773
Manabu Fujimoto: http://orcid.org/0000-0002-3062-4872
Dennis R. Roop: http://orcid.org/0000-0001-5868-5880
Akemi Ishida-Yamamoto: http://orcid.org/0000-0002-3104-102X

AUTHOR CONTRIBUTIONS

Conceptualization: YI; Data Curation: YI, OT, AIY; Formal Analysis: YI, AIY, DRR; Funding Acquisition: YI, YN, AS, YF, RW, NO, MF; Investigation: YI, AIY; Methodology: YI, TO, AIY; Project Administration: YI; Supervision: DRR, MF; Validation: YI, AIY; Visualisation: YI; Writing - Original Draft Preparation: YI; Writing - Review and Editing: YI, AIY, DRR

CONFLICT OF INTEREST

The authors state no conflict of interest.

ACKNOWLEDGMENTS

We would like to thank Yuriko Hirota and Hideko Sakurai for helping with the laboratory work. This research was supported in part by the following Japanese Society for the Promotion of Science KAKENHI grants (a Grant-in-Aid for Research Activity Start-Up) (16H06663 to YI) and an Early-Career Scientists Grant (18K16018 to YI).

REFERENCES

Allen M, Ishida-Yamamoto A, McGrath J, Davison S, Iizuka H, Simon M, et al. Corneodesmosin expression in psoriasis vulgaris differs from normal skin and other inflammatory skin disorders. Lab Invest 2001;81:969–76.

Descargues P, Deraison C, Bonnart C, Kreft M, Kishibe M, Ishida-Yamamoto A, et al. Spink5-deficient mice mimic netherton syndrome through degradation of desmoglein 1 by epidermal protease hyperactivity. Nat Genet 2005;37:56–65.

Dinkova-Kostova AT, Holtzclaw WD, Cole RN, Itoh K, Wakabayashi N, Katoh Y, et al. Direct evidence that sulfhydryl groups of Keap1 are the sensors regulating induction of phase 2 enzymes that protect against carcinogens and oxidants. Proc Natl Acad Sci USA 2002;99:11908–13.

Doran TI, Vidrich A, Sun TT. Intrinsic and extrinsic regulation of the differentiation of skin, corneal and esophageal epithelial cells. Cell 1980;22:17–25.

Eckhart L, Lippens S, Tschachler E, Declercq W. Cell death by cornification. Biochim Biophys Acta 2013;1833:3471–80.

Ehrlich F, Fischer H, Langbein L, Praetzel-Wunder S, Ebner B, Figlak K, et al. Differential evolution of the epidermal keratin cytoskeleton in terrestrial and aquatic mammals. Mol Biol Evol 2019;36:328–40.

Ghadially R, Reed JT, Elias PM. Stratum corneum structure and function correlates with phenotype in psoriasis. J Invest Dermatol 1996;107:558–64.

Gregorio J, Meller S, Conrad C, Di Nardo A, Homey B, Lauerma A, et al. Plasmacytoid dendritic cells sense skin injury and promote wound healing through type I interferons. J Exp Med 2010;207:2921–30.

Hohl D, Mehrel T, Lichti U, Turner ML, Roop DR, Steinert PM. Characterization of human loricrin. Structure and function of a new class of epidermal cell envelope proteins. J Biol Chem 1991;266:6626–36.

Huebner AJ, Dai D, Morasso M, Schmidt EE, Schäfer M, Werner S, et al. Amniotic fluid activates the nrf2/keap1 pathway to repair an epidermal barrier defect in utero. Dev Cell 2012;23:1238–46.

Igawa S, Kishibe M, Murakami M, Honma M, Takahashi H, Iizuka H, et al. Tight junctions in the stratum corneum explain spatial differences in corneodesmosome degradation. Exp Dermatol 2011;20:53–7.

Ishida-Yamamoto A, Deraison C, Bonnart C, Bitoun E, Robinson R, O'Brien TJ, et al. LEKTI is localized in lamellar granules, separated from KLK5 and KLK7, and is secreted in the extracellular spaces of the superficial stratum granulosum. J Invest Dermatol 2005;124:360–6.

Ishida-Yamamoto A, Eady RA, Watt FM, Roop DR, Hohl D, Iizuka H. Immunoelectron microscopic analysis of cornified cell envelope formation in normal and psoriatic epidermis. J Histochem Cytochem 1996;44:167–75.

Ishida-Yamamoto A, Igawa S, Kishibe M. Order and disorder in corneocyte adhesion. J Dermatol 2011;38:645–54.

Ishida-Yamamoto A, Igawa S, Kishibe M. Molecular basis of the skin barrier structures revealed by electron microscopy. Exp Dermatol 2018;27:841–6.

Ishida-Yamamoto A, Kato H, Kiyama H, Armstrong DK, Munro CS, Eady RA, et al. Mutant loricrin is not crosslinked into the cornified cell envelope but is translocated into the nucleus in loricrin keratoderma. J Invest Dermatol 2000;115:1088–94.

Ishitsuka Y, Huebner AJ, Rice RH, Koch PJ, Speransky VV, Steven AC, et al. Lce1 family members are Nrf2-target genes that are induced to compensate for the loss of loricrin. J Invest Dermatol 2016;136:1656–63.

Ishitsuka Y, Ogawa T, Roop D. The KEAP1/NRF2 signaling pathway in keratinization. Antioxidants (Basel) 2020;9:751.

Ishitsuka Y, Roop DR. Loricrin confers photoprotective function against UVB in corneocytes. J Invest Dermatol 2018;138:2684–7.

Ishitsuka Y, Roop DR. Loricrin: past, present, and future. Int J Mol Sci 2020;21:2271.

Itoh K, Chiba T, Takahashi S, Ishii T, Igarashi K, Katoh Y, et al. An Nrf2/small Maf heterodimer mediates the induction of phase II detoxifying enzyme genes through antioxidant response elements. Biochem Biophys Res Commun 1997;236:313–22.

Itoh K, Wakabayashi N, Katoh Y, Ishii T, Igarashi K, Engel JD, et al. Keap1 represses nuclear activation of antioxidant responsive elements by Nrf2 through binding to the amino-terminal Neh2 domain. Genes Dev 1999;13:76–86.

Jonca N, Guerrin M, Hadjiolova K, Caubet C, Gallinaro H, Simon M, et al. Corneodesmosin, a component of epidermal corneocyte desmosomes, displays homophilic adhesive properties. J Biol Chem 2002;277:5024–9.

Kalinin A, Marekov LN, Steinert PM. Assembly of the epidermal cornified cell envelope. J Cell Sci 2001;114:3069–70.

Kang MI, Kobayashi A, Wakabayashi N, Kim SG, Yamamoto M. Scaffolding of Keap1 to the actin cytoskeleton controls the function of Nrf2 as key regulator of cytoprotective phase 2 genes. Proc Natl Acad Sci USA 2004;101:2046–51.

Katoh Y, Iida K, Kang MI, Kobayashi A, Mizukami M, Tong KI, et al. Evolutionary conserved N-terminal domain of Nrf2 is essential for the Keap1-mediated degradation of the protein by proteasome. Arch Biochem Biophys 2005;433:342–50.

Kobayashi M, Itoh K, Suzuki T, Osanai H, Nishikawa K, Katoh Y, et al. Identification of the interactive interface and phylogenic conservation of the Nrf2-Keap1 system. Genes Cells 2002;7:807–20.

Koch PJ, de Viragh PA, Scharer E, Bundman D, Longley MA, Bickenbach J, et al. Lessons from loricrin-deficient mice: compensatory mechanisms maintaining skin barrier function in the absence of a major cornified envelope protein. J Cell Biol 2000;151:389–400.

Kuo IH, Carpenter-Mendini A, Yoshida T, McGirt LY, Ivanov AI, Barnes KC, et al. Activation of epidermal toll-like receptor 2 enhances tight junction function: implications for atopic dermatitis and skin barrier repair. J Invest Dermatol 2013;133:988–98.

Lavker RM, Matoltsy AG. Formation of horny cells: the fate of cell organelles and differentiation products in ruminal epithelium. J Cell Biol 1970;44:501–12.

Leclerc EA, Huchenq A, Mattiuzzo NR, Metzger D, Chambon P, Ghyselinck NB, et al. Corneodesmosin gene ablation induces lethal skin-barrier disruption and hair-follicle degeneration related to desmosome dysfunction. J Cell Sci 2009;122:2699–709.

Macdiarmid J, Wilson JB. Separation of epidermal tissue from underlying dermis and primary keratinocyte culture. Methods Mol Biol 2001;174:401–10.

Matsumoto M, Zhou Y, Matsuo S, Nakanishi H, Hirose K, Oura H, et al. Targeted deletion of the murine corneodesmosin gene delineates its essential role in skin and hair physiology. Proc Natl Acad Sci USA 2008;105:6720–4.

Mehrel T, Hohl D, Rothnagel JA, Longley MA, Bundman D, Cheng C, et al. Identification of a major keratinocyte cell envelope protein, loricrin. Cell 1990;61:1103–12.

Menon GK, Feingold KR, Elias PM. Lamellar body secretory response to barrier disruption. J Invest Dermatol 1992;98:279–89.

Michel S, Schmidt R, Shroot B, Reichert U. Morphological and biochemical characterization of the cornified envelopes from human epidermal keratinocytes of different origin. J Invest Dermatol 1988;91:11–5.

Mils V, Vincent C, Croute F, Serre G. The expression of desmosomal and corneodesmosomal antigens shows specific variations during the terminal differentiation of epidermis and hair follicle epithelia. J Histochem Cytochem 1992;40:1329–37.

Nemes Z, Steinert PM. Bricks and mortar of the epidermal barrier. Exp Mol Med 1999;31:5–19.

Ogawa T, Ishitsuka Y, Inoue S, Nakamura Y, Saito A, Okiyama N, et al. Nuclear factor erythroid 2-related factor 2 (Nrf2) regulates epidermal keratinization under psoriatic skin inflammation. Am J Pathol 2020a;190:577–85.

Ogawa T, Ishitsuka Y, Nakamura Y, Kubota N, Saito A, Fujisawa Y, et al. NRF2 augments epidermal antioxidant defenses and promotes atopy. J Immunol 2020b;205:907–14.

Rice RH, Durbin-Johnson BP, Ishitsuka Y, Salemi M, Phinney BS, Rocke DM, et al. Proteomic analysis of loricrin knockout mouse epidermis. J Proteome Res 2016;15:2560–6.

Rice RH, Green H. The cornified envelope of terminally differentiated human epidermal keratinocytes consists of cross-linked protein. Cell 1977;11:417–22.

Schäfer M, Farwanah H, Willrodt AH, Huebner AJ, Sandhoff K, Roop D, et al. Nrf2 links epidermal barrier function with antioxidant defense. EMBO Mol Med 2012;4:364–79.

Schäfer M, Werner S. Nrf2–a regulator of keratinocyte redox signaling. Free Radic Biol Med 2015;88:243–52.

Schäfer M, Willrodt AH, Kurinna S, Link AS, Farwanah H, Geusau A, et al. Activation of Nrf2 in keratinocytes causes chloracne (MADISH)-like skin disease in mice. EMBO Mol Med 2014;6:442–57.

Schulze-Topphoff U, Varrin-Doyer M, Pekarek K, Spencer CM, Shetty A, Sagan SA, et al. Dimethyl fumarate treatment induces adaptive and innate immune modulation independent of Nrf2. Proc Natl Acad Sci USA 2016;113:4777–82.

Serre G, Mils V, Haftek M, Vincent C, Croute F, Réano A, et al. Identification of late differentiation antigens of human cornified epithelia, expressed in re-organized desmosomes and bound to cross-linked envelope. J Invest Dermatol 1991;97:1061–72.

Sevilla LM, Nachat R, Groot KR, Klement JF, Uitto J, Djian P, et al. Mice deficient in involucrin, envoplakin, and periplakin have a defective epidermal barrier. J Cell Biol 2007;179:1599–612.

Simon M, Green H. Participation of membrane-associated proteins in the formation of the cross-linked envelope of the keratinocyte. Cell 1984;36:827–34.

Simon M, Jonca N, Guerrin M, Haftek M, Bernard D, Caubet C, et al. Refined characterization of corneodesmosin proteolysis during terminal differentiation of human epidermis and its relationship to desquamation [published correction appears in J Biol Chem 2001;276:47742–3]. J Biol Chem 2001;276:20292–9.

Simon M, Montézin M, Guerrin M, Durieux JJ, Serre G. Characterization and purification of human corneodesmosin, an epidermal basic glycoprotein associated with corneocyte-specific modified desmosomes. J Biol Chem 1997;272:31770–6.

Simon M, Tazi-Ahnini R, Jonca N, Caubet C, Cork MJ, Serre G. Alterations in the desquamation-related proteolytic cleavage of corneodesmosin and other corneodesmosomal proteins in psoriatic lesional epidermis. Br J Dermatol 2008;159:77–85.

Steinert PM, Candi E, Kartasova T, Marekov L. Small proline-rich proteins are cross-bridging proteins in the cornified cell envelopes of stratified squamous epithelia. J Struct Biol 1998;122:76–85.

Steinert PM, Marekov LN. The proteins elafin, filaggrin, keratin intermediate filaments, loricrin, and small proline-rich proteins 1 and 2 are isodipeptide cross-linked components of the human epidermal cornified cell envelope. J Biol Chem 1995;270:17702–11.

Suga Y, Jarnik M, Attar PS, Longley MA, Bundman D, Steven AC, et al. Transgenic mice expressing a mutant form of loricrin reveal the molecular basis of the skin diseases, Vohwinkel syndrome and progressive symmetric erythrokeratoderma. J Cell Biol 2000;151:401–12.

Swartzendruber DC, Wertz PW, Madison KC, Downing DT. Evidence that the corneocyte has a chemically bound lipid envelope. J Invest Dermatol 1987;88:709–13.

Van Scott EJ, Flesch P. Sulfhydryl disulfide in keratinization. Science 1954;119:70–1.

Vermeij WP, Alia A, Backendorf C. ROS quenching potential of the epidermal cornified cell envelope. J Invest Dermatol 2011;131:1435–41.

Vermeij WP, Backendorf C. Skin cornification proteins provide global link between ROS detoxification and cell migration during wound healing. PLoS One 2010;5:e11957.

Wakabayashi N, Itoh K, Wakabayashi J, Motohashi H, Noda S, Takahashi S, et al. Keap1-null mutation leads to postnatal lethality due to constitutive Nrf2 activation. Nat Genet 2003;35:238–45.

Williamson MP. The structure and function of proline-rich regions in proteins. Biochem J 1994;297:249–60.

Wood W, Jacinto A, Grose R, Woolner S, Gale J, Wilson C, et al. Wound healing recapitulates morphogenesis in Drosophila embryos. Nat Cell Biol 2002;4:907–12.

Yamamoto M, Kensler TW, Motohashi H. The KEAP1-NRF2 system: a thiol-based sensor-effector apparatus for maintaining redox homeostasis. Physiol Rev 2018;98:1169–203.

Zuo Y, Zhuang DZ, Han R, Isaac G, Tobin JJ, McKee M, et al. ABCA12 maintains the epidermal lipid permeability barrier by facilitating formation of ceramide linoleic esters. J Biol Chem 2008;283:36624–35.